PHYSICAL REVIEW D 92, 094004 (2015)

Polyakov loop fluctuations in the Dirac eigenmode expansion

Takahiro M. Doi,[1] Krzysztof Redlich,[2,3,4] Chihiro Sasaki,[2,5] and Hideo Suganuma[1]

[1]*Department of Physics, Kyoto University, Kyoto 606-8502, Japan*
[2]*Institute of Theoretical Physics, University of Wroclaw, PL-50204 Wroclaw, Poland*
[3]*Extreme Matter Institute EMMI, GSI, Planckstrasse 1, D-64291 Darmstadt, Germany*
[4]*Department of Physics, Duke University, Durham, North Carolina 27708, USA*
[5]*Frankfurt Institute for Advanced Studies, D-60438 Frankfurt am Main, Germany*

(Received 21 May 2015; published 3 November 2015)

We investigate correlations of the Polyakov loop fluctuations with eigenmodes of the lattice Dirac operator. Their analytic relations are derived on the temporally odd-number size lattice with the normal nontwisted periodic boundary condition for the link variables. We find that the low-lying Dirac modes yield negligible contributions to the Polyakov loop fluctuations. This property is confirmed to be valid in confined and deconfined phases by numerical simulations in SU(3) quenched QCD. These results indicate that there is no direct, one-to-one correspondence between confinement and chiral symmetry breaking in QCD in the context of different properties of the Polyakov loop fluctuation ratios.

DOI: 10.1103/PhysRevD.92.094004 PACS numbers: 12.38.Aw, 12.38.Gc, 14.70.Dj

I. INTRODUCTION

Color confinement and chiral symmetry breaking are the striking nonperturbative phenomena in low-energy QCD, which are of particular importance in particle and nuclear physics [1–5].

Several scenarios of the confinement mechanism have been proposed [3–8] in which the ghost and gluon propagators in the deep infrared need to be quantified; thus, this requires a nonperturbative quantization of QCD. Whereas this issue has been investigated extensively, it remains challenging to comprehend the nonperturbative aspects from the first-principle calculations.

In a pure SU(3) gauge theory, the Polyakov loop is an exact order parameter of the Z_3 center symmetry and for deconfinement, which dictates a first-order phase transition [3,9–11]. In the presence of light dynamical quarks, the Polyakov loop loses its interpretation as an order parameter and is smoothly changing with temperature. However, contrary to the broad Polyakov loop, a particular ratio of the Polyakov loop susceptibilities retains a clear remnant of the underlying Z_3 center symmetry fairly well even in full QCD with the physical pion mass [12,13]. Thus, the ratio of the Polyakov loop fluctuations can serve as observables to identify the onset of deconfinement in QCD.

In the presence of light dynamical quarks, the transition from the hadronic phase to quark-gluon plasma becomes a crossover and accompanies the partial restoration of chiral symmetry at a finite temperature [14–16]. Spontaneous chiral symmetry breaking is characterized by a nonvanishing condensation of quark-bilinear operators. The low-lying Dirac modes, which are the eigenmodes of the Dirac operator with small eigenvalues, are known to be responsible for saturating the chiral condensate of light quarks $\langle\bar{\psi}\psi\rangle$, through the Banks–Casher relation [17].

In fact, at vanishing and small baryon chemical potentials, the lattice QCD results suggest that there is an interplay between quark deconfinement and chiral crossovers as they take place in the same narrow temperature range [18]. Also, in the maximally Abelian gauge, confinement, chiral symmetry breaking, and instantons simultaneously disappear, when the QCD monopoles are removed [19–22]. On the other hand, there exist several observations that unbroken chiral symmetry does not dictate deconfinement: given a tower of hadron spectra with eliminating the low-lying Dirac modes [23], the hadrons keep their identity even in a chirally restored phase where parity doublers are all degenerate. In addition, it has been shown in the SU(3) lattice simulations that the low-lying modes have little contribution to the Polyakov loop and to the confining force, indicating that the two features are rather independent [24–26].

In the context of the interplay between confinement and chiral symmetry breaking [15,18,20,21,23–30], it is important to make a reliable separation of one from another, whereas those phenomena are supposed to be correlated. The apparent coincidence in the change of properties of the Polyakov loop fluctuation ratios and the chiral condensate and its susceptibility near the chiral crossover might indicate that there is a tied relation between the confinement and chiral symmetry breaking in QCD. However, such a possible relation has not been quantified yet.

Utilizing the Dirac-mode expansion method formulated on the lattice [24], the low-lying modes can be systematically removed in calculating expectation values of different operators.

In this paper, we apply the above expansion method to investigate the relation between confinement and chiral symmetry breaking in terms of the Polyakov loop fluctuations and their ratios. We pay particular attention to the contribution of the low-lying Dirac modes to the Polyakov loop fluctuations.

We derive the analytic relations between the real and imaginary parts and modulus of the Polyakov loop and their fluctuations with the Dirac modes on the temporally odd-number size lattice with periodic boundary conditions. These analytical relations are applicable to both full and quenched QCD. We show, through numerical simulations on the lattice in quenched QCD, that the low-lying Dirac modes yield negligible contribution to the Polyakov loop fluctuations. With these results, also not observed is a direct relation between confinement and chiral symmetry breaking in QCD through the Polyakov loop fluctuation ratios.

The paper is organized as follows. In the next section, we derive a set of analytic relations linking the Polyakov loop fluctuations to the Dirac eigenmodes. In Sec. III, we examine the role of the low-lying Dirac modes in the Polyakov loop fluctuations and present our numerical results within quenched lattice QCD. Section IV is devoted to a summary and conclusions.

II. POLYAKOV LOOP FLUCTUATIONS

We utilize the $\mathrm{SU}(N_c)$ lattice QCD formalism and consider a square lattice with spacing a. Each site is indicated by $s = (s_1, s_2, s_3, s_4)$ with $s_\mu = 1, 2, \ldots, N_\mu$. A gauge field, $A_\mu(s) \in \mathrm{SU}(N_c)$ with the gauge coupling g, is introduced as a link variable, $U_\mu(s) = \mathrm{e}^{iagA_\mu(s)}$. We use the spatially symmetric lattice, i.e., $N_1 = N_2 = N_3 \equiv N_\sigma$ and $N_4 \equiv N_\tau$, with $N_\sigma \geq N_\tau$.

For each gauge configuration, the Polyakov loop L is defined as

$$L \equiv \frac{1}{N_c V} \sum_s \mathrm{tr}_c \left\{ \prod_{i=0}^{N_\tau - 1} U_4(s + i\hat{4}) \right\}, \tag{1}$$

where $\hat{\mu}$ is the unit vector in the direction of μ in the lattice unit and V is the four-dimensional lattice volume, $V = N_\sigma^3 N_\tau$.

Under the Z_3 rotation, the Polyakov loop is transformed into

$$\tilde{L} = L\mathrm{e}^{2\pi k i/3} \tag{2}$$

with $k = 0, \pm 1$ [12,13]. In the confined phase, $k = 0$ is taken. In the deconfined phase, k is chosen such that the transformed Polyakov loop $\tilde{L}$ lies in its real sector.

We introduce the Polyakov loop susceptibilities,

$$T^3 \chi_A = \frac{N_\sigma^3}{N_\tau^3} [\langle |L|^2 \rangle - \langle |L| \rangle^2], \tag{3}$$

$$T^3 \chi_L = \frac{N_\sigma^3}{N_\tau^3} [\langle (L_L)^2 \rangle - \langle L_L \rangle^2], \tag{4}$$

$$T^3 \chi_T = \frac{N_\sigma^3}{N_\tau^3} [\langle (L_T)^2 \rangle - \langle L_T \rangle^2], \tag{5}$$

where $L_L \equiv \mathrm{Re}(\tilde{L})$ and $L_T \equiv \mathrm{Im}(\tilde{L})$, and consider their ratios,

$$R_A \equiv \frac{\chi_A}{\chi_L}, \tag{6}$$

$$R_T \equiv \frac{\chi_T}{\chi_L}. \tag{7}$$

The Polyakov loop susceptibility ratios (6) and (7) were shown to be excellent probes of the deconfinement phase transition in a pure gauge theory [12,13]. They are almost temperature independent above and below the transition and exhibit a discontinuity at the transition temperature. This characteristic behavior is understood in terms of the global Z_3 symmetry of the Yang–Mills Lagrangian and the general properties of the Polyakov loop probability distribution [12].

In the presence of dynamical quarks, the Polyakov loop is no longer an order parameter and stays finite even in the low-temperature phase. Consequently, the ratios of the Polyakov loop susceptibilities are modified due to explicit breaking of the Z_3 center symmetry. Indeed, both R_A and R_T vary continuously with the temperature across the chiral crossover; however, R_A interpolates between the two limiting values set by the pure gauge theory. This property of R_A is illustrated in Fig. 1. Also seen in this figure is that, in spite of smoothening effects observed in the presence of quarks, there is an abrupt rate change with T in R_A near the chiral crossover $T \simeq 155$ MeV [13]. The ratio R_A in Fig. 1 has its inflection point at $T \simeq 150$ MeV, which is fairly in good agreement with the chiral crossover range calculated in lattice QCD. Such behavior of the Polyakov loop

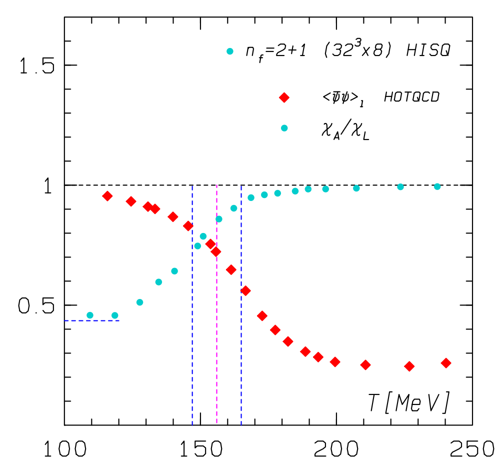

FIG. 1 (color online). The temperature dependence of the Polyakov loop susceptibilities ratio $R_A = \chi_A/\chi_T$ from Eq. (6) and the chiral condensate of light quarks $\langle\bar{\psi}\psi\rangle_l$, normalized to its zero-temperature value. The lattice QCD Monte Carlo results are from Refs. [13] and [31], respectively. The horizontal dashed lines are the limiting values of R_A in a pure SU(3) lattice gauge theory [12]. The vertical dashed lines indicate the chiral crossover temperature and the range of its errors [31–33].

fluctuation ratio can be regarded as an effective observable indicating deconfinement properties in QCD [13].

The apparent modification of R_A and R_T near the chiral crossover may suggest that there are certain correlations between the confinement and chiral symmetry breaking. Such correlations can be best verified when expanding the Polyakov loop and its fluctuations in terms of the Dirac eigenmodes.

In the following, we formulate the relevant quantities, based on this expansion method, and study the influence of the low-lying Dirac modes on the properties of the Polyakov loop fluctuation ratios.

III. DIRAC-MODE EXPANSION

To derive the analytic relation between the Polyakov loop and the Dirac modes, we consider the temporally odd-number lattice with the normal nontwisted periodic boundary condition for link variables, in both temporal and spatial directions [25,26].

We introduce the link-variable operator $\hat{U}_{\pm\mu}$, with the matrix element

$$\langle s|\hat{U}_{\pm\mu}|s'\rangle = U_{\pm\mu}(s)\delta_{s\pm\hat{\mu},s'}. \tag{8}$$

The covariant derivative operator on the lattice is introduced as

$$\hat{D}_\mu = \frac{1}{2a}(\hat{U}_\mu - \hat{U}_{-\mu}), \tag{9}$$

and the Dirac operator

$$\hat{\not{D}} = \gamma_\mu \hat{D}_\mu = \frac{1}{2a}\sum_{\mu=1}^{4}\gamma_\mu(\hat{U}_\mu - \hat{U}_{-\mu}), \tag{10}$$

with its matrix element

$$\not{D}_{s,s'} = \frac{1}{2a}\sum_{\mu=1}^{4}\gamma_\mu[U_\mu(s)\delta_{s+\hat{\mu},s'} - U_{-\mu}(s)\delta_{s-\hat{\mu},s'}], \tag{11}$$

where $U_{-\mu}(s) = U_\mu^\dagger(s-\hat{\mu})$ and $\gamma_\mu^\dagger = \gamma_\mu$.

Since the Dirac operator is anti-Hermitian, the Dirac eigenvalue equation reads

$$\hat{\not{D}}|n\rangle = i\lambda_n|n\rangle, \tag{12}$$

where $\lambda_n \in \mathbf{R}$. Using the Dirac eigenfunction $\psi_n(s) \equiv \langle s|n\rangle$, one arrives at the eigenvalue equation

$$\frac{1}{2a}\sum_{\mu=1}^{4}\gamma_\mu[U_\mu(s)\psi_n(s+\hat{\mu}) - U_{-\mu}(s)\psi_n(s-\hat{\mu})] = i\lambda_n\psi_n(s). \tag{13}$$

At finite temperature, imposing the temporal antiperiodicity for $\hat{D}_4$ acting on quarks, it is convenient to add a minus sign to the matrix element of the temporal link-variable operator $\hat{U}_{\pm 4}$ at the temporal boundary of $t = N_t (=0)$ [25]:

$$\begin{aligned}\langle \mathbf{s}, N_t|\hat{U}_4|\mathbf{s}, 1\rangle &= -U_4(\mathbf{s}, N_t),\\ \langle \mathbf{s}, 1|\hat{U}_{-4}|\mathbf{s}, N_t\rangle &= -U_{-4}(\mathbf{s}, 1) = -U_4^\dagger(\mathbf{s}, N_t).\end{aligned} \tag{14}$$

Then, the Polyakov loop in Eq. (1) is expressed as

$$L = -\frac{1}{N_c V}\mathrm{Tr}_c\{\hat{U}_4^{N_\tau}\} = \frac{1}{N_c V}\sum_s \mathrm{tr}_c\left\{\prod_{n=0}^{N_t-1} U_4(s+n\hat{t})\right\}, \tag{15}$$

where Tr_c denotes the functional trace, $\mathrm{Tr}_c \equiv \sum_s \mathrm{tr}_c$, and tr_c is taken over the color index. The minus sign stems from the additional minus on $U_4(\mathbf{s}, N_t)$ in Eq. (14).

Note that the functional trace of a product of link-variable operators corresponding to nonclosed path is exactly zero. Indeed, followed by Eq. (8), one obtains

$$\begin{aligned}&\mathrm{Tr}_c(\hat{U}_{\mu_1}\hat{U}_{\mu_2}\ldots\hat{U}_{\mu_{N_P}})\\ &= \mathrm{tr}_c\sum_s \langle s|\hat{U}_{\mu_1}\hat{U}_{\mu_2}\ldots\hat{U}_{\mu_{N_P}}|s\rangle\\ &= \mathrm{tr}_c\sum_s U_{\mu_1}(s)\ldots U_{\mu_{N_P}}\left(s+\sum_{k=1}^{N_P-1}\hat{\mu}_k\right)\\ &\quad\times\left\langle s+\sum_{k=1}^{N_P}\hat{\mu}_k|s\right\rangle = 0,\end{aligned} \tag{16}$$

with $\sum_{k=1}^{N_P}\hat{\mu}_k \neq 0$ for any nonclosed path of length N_P. This is understood from Elitzur's theorem [34] that the vacuum expectation values of gauge-variant operators are zero.

In the following, we show that the Polyakov loop can be explicitly expanded in terms of eigenmodes of the Dirac operator.

A. Relation between the Polyakov loop and Dirac modes

We introduce the key quantity

$$I = \mathrm{Tr}_{c,\gamma}(\hat{U}_4\hat{\not{D}}^{N_\tau-1}), \tag{17}$$

where $\mathrm{Tr}_{c,\gamma} \equiv \sum_s \mathrm{tr}_c\mathrm{tr}_\gamma$ and tr_γ is taken over spinor indices. From the definition of $\hat{\not{D}}$ in Eq. (10), it is clear that the

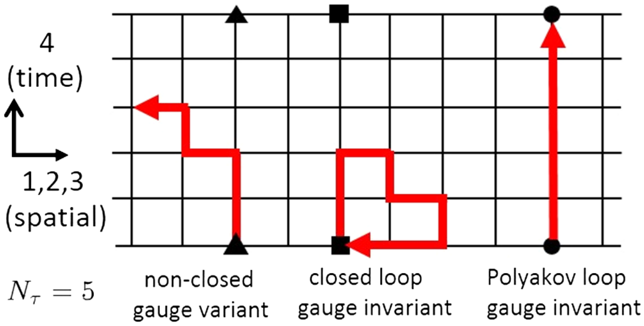

FIG. 2 (color online). The link path structure on a temporally odd-number lattice with $N_\tau = 5$ and with the periodic boundary condition. The left configuration is gauge variant, whereas the middle is gauge invariant. The right configuration represents a closed path with N_τ (link variables) because of the periodicity in a temporal direction, and thus this path corresponds to a gauge-invariant Polyakov loop.

$\hat{U}_4\hat{\not{D}}^{N_\tau-1}$ operator is expressed by a sum of products of N_τ (link variables).

Note that, on a square lattice, it is not possible to construct any closed loop using the products of an odd number of link variables (see Fig. 2 for an illustration). By construction, one considers a square lattice with odd N_τ, and thus $\hat{U}_4\hat{\not{D}}^{N_\tau-1}$ in Eq. (17) does not contain any contributions from the products of N_τ (link variables) along the closed paths. However, due to the periodic boundary condition in the time direction, the only exception is a gauge-invariant term proportional to $\hat{U}_4^{N_\tau}$. This term is thus related with the Polyakov loop operator.

Based on the above discussion, and applying Eqs. (15), (16), and (9) to Eq. (17), one finds that

$$I = \frac{12V}{(2a)^{N_\tau-1}} L, \tag{18}$$

and thus I is directly proportional to the Polyakov loop.

On the other hand, since I in Eq. (17) is defined through the functional trace, it can be expressed in the basis of Dirac eigenmodes as

$$\begin{aligned} I &= \sum_n \langle n|\hat{U}_4\hat{\not{D}}^{N_\tau-1}|n\rangle \\ &= i^{N_\tau-1}\sum_n \lambda_n^{N_\tau-1}\langle n|\hat{U}_4|n\rangle. \end{aligned} \tag{19}$$

Consequently, from Eqs. (18) and (19), one finds that, on the temporally odd-number lattice, there is a direct relation between the Polyakov loop and the Dirac modes [25,26],

$$L = \frac{(2ai)^{N_\tau-1}}{12V}\sum_n \lambda_n^{N_\tau-1}\langle n|\hat{U}_4|n\rangle, \tag{20}$$

which is a Dirac spectral representation of the Polyakov loop.

The relation (20) is a mathematical identity and is exactly satisfied for arbitrary gauge configurations. Consequently, this relation is valid, regardless of whether the link variables are generated in full QCD or quenched QCD [25].

The relation (20) enables us to investigate the contribution of different Dirac modes to the Polyakov loop. Of particular interest is the role of the low-lying eigenvalues which are essential to identify chiral symmetry restoration in QCD at a finite temperature.

In principle, it is possible to calculate numerically the contribution of the Dirac modes to the Polyakov loop through Eq. (20) by using Monte Carlo simulations. However, a very large $(4\times N_c\times V)^2$ dimension of a Dirac operator implies also a large cost of numerical calculations. This can be, however, remarkably reduced by the use of the modified Kogut–Susskind (KS) formalism [26].

We rewrite Eq. (20) into the equivalent form

$$L = \frac{(2ai)^{N_\tau-1}}{3V}\sum_n \lambda_n^{N_\tau-1}(n|\hat{U}_4|n), \tag{21}$$

where the KS Dirac eigenstate $|n)$ is obtained by solving the eigenvalue equation,

$$\eta_\mu D_\mu|n) = i\lambda_n|n). \tag{22}$$

Here, the KS Dirac operator $\eta_\mu D_\mu$ is defined as

$$(\eta_\mu D_\mu)_{ss'} = \frac{1}{2a}\sum_{\mu=1}^{4}\eta_\mu(s)[U_\mu(s)\delta_{s+\hat{\mu},s'} - U_{-\mu}(s)\delta_{s-\hat{\mu},s'}] \tag{23}$$

with the staggered phase $\eta_\mu(s)$,

$$\eta_1(s) \equiv 1, \qquad \eta_\mu(s) \equiv (-1)^{s_1+\cdots+s_{\mu-1}}(\mu\geq 2). \tag{24}$$

Consequently, each Dirac-mode contribution to the Polyakov loop is obtained by solving the eigenvalue equation of the KS Dirac operator of which the dimension is now $(N_c\times V)^2$, instead of $(4\times N_c\times V)^2$, as in the original Dirac operator.

In terms of the KS Dirac eigenfunction $\chi_n(s) = \langle s|n)$, the KS Dirac matrix element $(n|\hat{U}_\mu|m)$ is explicitly expressed as

$$\begin{aligned} (n|\hat{U}_\mu|m) &= \sum_s (n|s\rangle\langle s|\hat{U}_\mu|s+\hat{\mu}\rangle\langle s+\hat{\mu}|m) \\ &= \sum_s \chi_n(s)^\dagger U_\mu(s)\chi_m(s+\hat{\mu}). \end{aligned} \tag{25}$$

From the gauge transformation property of link variables and the KS Dirac eigenfunctions, the matrix element $(n|\hat{U}_\mu|m)$ is gauge invariant [25,26].

Note that the modified KS formalism applied here is not an approximation but is a method for spin diagonalization of the Dirac operator. In this study, we do not use specific fermions, such as the KS fermion, but apply the modified KS formalism as a prescription to reduce the numerical cost.

The relations of the Polyakov loop and Dirac eigenmodes in Eqs. (20) and (21) are exact. They are valid at finite temperature and density and are independent of the particular implementation of fermions on the lattice [25] and thus can be used to identify the interplay between deconfinement and chiral symmetry restoration in QCD.

B. Polyakov loop fluctuations and Dirac modes

The expansion of the Polyakov loop in terms of the Dirac eigenmodes, formulated in the previous section, can be also applied to the fluctuations of the real and imaginary parts and modulus of the Polyakov loop.

Multiplying Eq. (20) by the Z_3 factor $\mathrm{e}^{2\pi ki/3}$, one obtains the relation between the Z_3 transformed Polyakov loop $\tilde{L}$ and the Dirac modes,

$$\tilde{L} = \frac{(2ai)^{N_\tau-1}}{12V}\sum_n \lambda_n^{N_\tau-1}\mathrm{e}^{2\pi ki/3}\langle n|\hat{U}_4|n\rangle, \tag{26}$$

where $k = 0, \pm 1$ is chosen such that, for each gauge configuration, the $\tilde{L}$ lies in a real sector.

Taking the real and the imaginary parts of Eq. (26), the Dirac spectral representation of the longitudinal and transverse Polyakov loops reads

$$L_L = \frac{(2ai)^{N_\tau-1}}{12V}\sum_n \lambda_n^{N_\tau-1}\mathrm{Re}(\mathrm{e}^{2\pi ki/3}\langle n|\hat{U}_4|n\rangle), \tag{27}$$

$$L_T = \frac{(2ai)^{N_\tau-1}}{12V}\sum_n \lambda_n^{N_\tau-1}\mathrm{Im}(\mathrm{e}^{2\pi ki/3}\langle n|\hat{U}_4|n\rangle), \tag{28}$$

respectively, whereas, taking the absolute value of Eq. (20), the following relation is also obtained:

$$|L| = \frac{(2a)^{N_\tau-1}}{12V}\left|\sum_n \lambda_n^{N_\tau-1}\langle n|\hat{U}_4|n\rangle\right|. \tag{29}$$

Since Eqs. (26), (27), (28), and (29) are valid for each gauge configuration, the Dirac spectral representation for different fluctuations of the Polyakov loop and their ratios are directly obtained by substituting Eqs. (27)–(29) to Eqs. (3)–(5). As an example, we quote an explicit expression for the Dirac spectral representation of the $R_A = \chi_A/\chi_L$ ratio as

$$R_A = \frac{\langle|\sum_n \lambda_n^{N_\tau-1}\langle n|\hat{U}_4|n\rangle|^2\rangle - \langle|\sum_n \lambda_n^{N_\tau-1}\langle n|\hat{U}_4|n\rangle|\rangle^2}{\langle(\sum_n \lambda_n^{N_\tau-1}\mathrm{Re}(\mathrm{e}^{2\pi ki/3}\langle n|\hat{U}_4|n\rangle))^2\rangle - \langle\sum_n \lambda_n^{N_\tau-1}\mathrm{Re}(\mathrm{e}^{2\pi ki/3}\langle n|\hat{U}_4|n\rangle)\rangle^2}, \tag{30}$$

where $\langle x\rangle$ denotes an average over all gauge configurations.

The explicit analytic relations of the Dirac spectral decomposition of the real and imaginary parts and modulus of the Polyakov loops and their fluctuations are the key results of our studies. Note here that, like Eq. (20), these relations (26)–(29) are applicable to both full and quenched QCD, since we just use Elitzur's theorem [34]: only gauge-invariant quantities survive. All these relations are derived on the temporally odd-number lattice for practical reasons. However, a particular choice of the parity for the lattice size in the time direction does not alter the physics, since in the continuum limit, $a \to 0$ and $N_\tau \to \infty$, any number of large N_τ should give the same result [25,26]. In fact, similar relations are derived also on the even lattice, whereas a more compact form can be obtained on the temporally odd-number lattice [25,26]. It is, however, difficult to take the continuum extrapolation. For instance, the continuum limit of the Polyakov loop itself is still unsettled because of the uncertainty of its renormalization. However, at least, the ambiguity of the multiplicative renormalization of the Polyakov loop can be avoided by considering the ratio of the Polyakov loop susceptibilities [12,13].

IV. NUMERICAL RESULTS

To study numerically the influence of different Dirac modes on the Polyakov loop fluctuations and their ratios, we further apply the modified KS formalism. This amounts to replacing the diagonal Dirac matrix element $\langle n|\hat{U}_4|n\rangle$ in Eqs. (27)–(29) by the corresponding KS Dirac matrix element $(n|\hat{U}_4|n)$ [26], as

$$\langle n|\hat{U}_4|n\rangle = 4(n|\hat{U}_4|n). \tag{31}$$

We analyze the contributions from the low-lying Dirac modes to the Polyakov loop fluctuations in the SU(3) lattice QCD through Monte Carlo simulations. In the mathematical sense, all the obtained relations (26)–(29) hold for both full and quenched QCD. In this paper, we perform SU(3) lattice QCD calculations with the standard plaquette action at the quenched level on the $10^3 \times 5$-size lattice. Numerical studies are carried out both in the confined and deconfined phases for different couplings $\beta = \frac{2N_c}{g^2}$ and the corresponding temperatures, $T = 1/(N_\tau a)$. We use the Linear Algebra PACKage (LAPACK) [35] in diagonalizing the KS Dirac operator to obtain the eigenvalues λ_n and the eigenfunctions

$\chi_n(s)$. The lattice spacing a is determined by the zero-temperature string tension of $\sigma = 0.89$ GeV/fm on a large lattice at each $\beta = 6/g^2$. In fact, we calculate here the static quark-antiquark potential $V(r)$ on the 16^4 lattice at each β and fit it by the Cornell potential, i.e., the Coulomb plus linear form [3], to extract the string tension σ.

In the confined phase, we fix $\beta = 5.6$ on the $10^3 \times 5$ lattice, which corresponds to $a \simeq 0.25$ fm and $T \simeq 160$ MeV. We also calculate the Creutz ratio $\chi(3,3) \simeq 0.35(2)$, for an estimate of the string tension or the lattice spacing on the precise lattice [3,36], in spite of an additional contamination from the Coulomb potential. Nevertheless, this value is consistent with the string tension σ obtained from the potential $V(r)$ and leads to $a \simeq 0.28$ fm. Here, the average plaquette value is obtained as $\langle U_{\mu\nu}\rangle = 0.53(2)$, which is consistent with the previous SU(3) lattice studies [36]. In deconfined phase, the simulations are performed at $\beta = 6.0$ on the $10^3 \times 5$ lattice, i.e., for $a \simeq 0.1$ fm and $T \simeq 400$ MeV. On this lattice, the average plaquette value is $\langle U_{\mu\nu}\rangle = 0.60(2)$, which is also consistent with the previous works [36]. For each value of β, we use 20 gauge configurations, which are taken every 500 sweeps after the thermalization of 5000 sweeps.

Since the Polyakov loop and its different fluctuations are expressed as the sums over all Dirac modes, we divide the entire tower of the Dirac eigenvalues into the low- and higher-lying modes with the insertion of the infrared cutoff Λ.

Based on Eq. (21), we introduce the Λ-dependent Polyakov loops,

$$|L|_\Lambda = \frac{(2a)^{N_\tau - 1}}{3V}\left|\sum_{|\lambda_n|>\Lambda} \lambda_n^{N_\tau - 1}(n|\hat{U}_4|n)\right| \tag{32}$$

for the modulus and

$$(L_L)_\Lambda = C_\tau \sum_{|\lambda_n|>\Lambda} \lambda_n^{N_\tau - 1}\mathrm{Re}(\mathrm{e}^{2\pi k i/3}(n|\hat{U}_4|n)), \tag{33}$$

$$(L_T)_\Lambda = C_\tau \sum_{|\lambda_n|>\Lambda} \lambda_n^{N_\tau - 1}\mathrm{Im}(\mathrm{e}^{2\pi k i/3}(n|\hat{U}_4|n)) \tag{34}$$

for the real and the imaginary parts, respectively, with $C_\tau = (2ai)^{N_\tau - 1}/3V$.

Applying the cutoff-dependent Polyakov loops from Eqs. (32), (33), and (34) to Eqs. (3)–(5), we also introduce the Λ-dependent susceptibilities

$$T^3(\chi)_\Lambda = \frac{N_\sigma^3}{N_\tau^3}[\langle Y_\Lambda^2\rangle - \langle Y_\Lambda\rangle^2], \tag{35}$$

where Y stands for $|L|$, L_L, or L_T, and their ratios

$$(R_A)_\Lambda = \frac{(\chi_A)_\Lambda}{(\chi_L)_\Lambda}, \qquad (R_T)_\Lambda = \frac{(\chi_T)_\Lambda}{(\chi_L)_\Lambda}. \tag{36}$$

To differentiate the importance of the low-lying Dirac modes on the properties of the Polyakov loop fluctuations and the chiral condensate, we introduce the cutoff-dependent chiral condensate $\langle\bar\psi\psi\rangle_\Lambda$. In terms of the Dirac modes, the $\langle\bar\psi\psi\rangle_\Lambda$ is expressed as [24]

$$\langle\bar\psi\psi\rangle_\Lambda = -\frac{1}{V}\sum_{|\lambda_n|\geq\Lambda}\frac{2m}{\lambda_n^2 + m^2}, \tag{37}$$

where m is the current quark mass.

The chiral condensate is strongly affected by the low-lying Dirac modes. Taking a typical value for the infrared cutoff $\Lambda \simeq 0.4$ GeV and the quark mass $m \simeq 5$ MeV leads to a drastic reduction of the chiral condensate,

$$R_{\mathrm{chiral}} = \frac{\langle\bar\psi\psi\rangle_\Lambda}{\langle\bar\psi\psi\rangle} \simeq 0.02, \tag{38}$$

in a confined phase at $T \simeq 0$ [24,26].

Figure 3 shows the Dirac eigenvalue distribution $\rho(\lambda) = 1/V\sum_n\langle\delta(\lambda - \lambda_n)\rangle$ in the confined ($\beta = 5.6$) and deconfined ($\beta = 6.0$) phases. Note here that the near-zero Dirac-mode density $\rho(\lambda \simeq 0)$ is apparently finite in the confined phase, whereas it is highly suppressed in the deconfined phase. We show in Fig. 4 the bare chiral condensate $|\langle\bar\psi\psi\rangle|$ per a flavor in the confined phase as a function of the quark

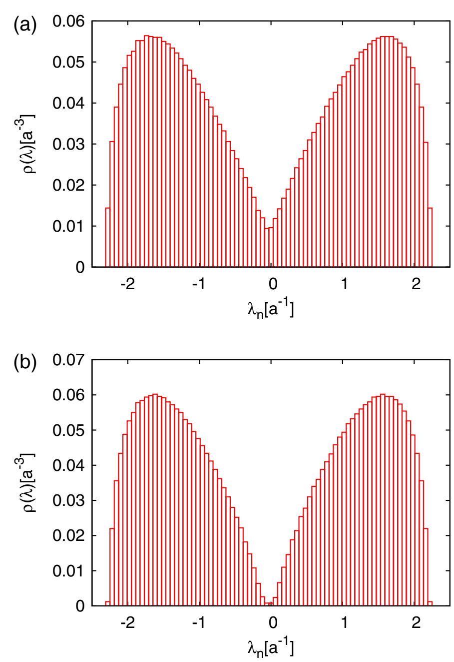

FIG. 3 (color online). The lattice QCD result of the Dirac eigenvalue distribution $\rho(\lambda)$ in the lattice unit: (a) the confinement phase at $\beta = 5.6$ (i.e., $a \simeq 0.25$ fm) on $10^3 \times 5$; (b) the deconfinement phase at $\beta = 6.0$ (i.e., $a \simeq 0.10$ fm) on $10^3 \times 5$ [26].

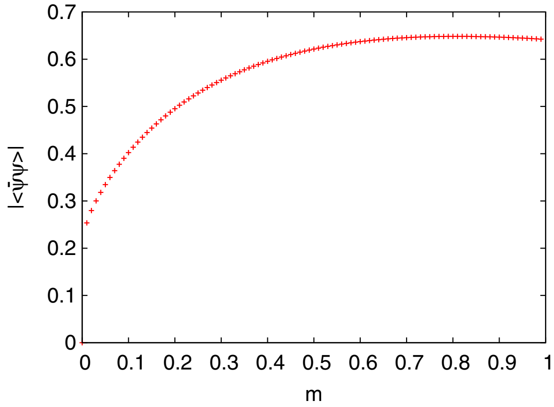

FIG. 4 (color online). The absolute value of the bare chiral condensate $|\langle\bar{\psi}\psi\rangle|$ per a flavor in the confinement phase plotted against the quark mass m in the lattice unit. The lattice QCD calculation is done at $\beta = 5.6$ (i.e., $a \simeq 0.25$ fm) on $10^3 \times 5$.

mass m in the lattice unit. The chiral condensate remains finite in the small-m region. Thus, from Figs. 3 and 4, it is clear that the chiral symmetry is definitely broken in the confined phase, whereas it is restored in the deconfined phase.

In the same spirit, we introduce the ratio,

$$R_{\mathrm{conf}} = \frac{(R_A)_\Lambda}{R_A}, \tag{39}$$

to quantify the sensitivity of the Polyakov loop fluctuations to the particular Dirac modes. When, with some Λ, the ratio stays $R_{\mathrm{conf}} \simeq 1$, then the low-lying Dirac modes below the cutoff Λ have a negligible contribution to the Polyakov loop fluctuations.

In Fig. 5, we show the Monte Carlo results for R_{conf} in a confined phase at $\beta = 5.6$, for various values of the infrared

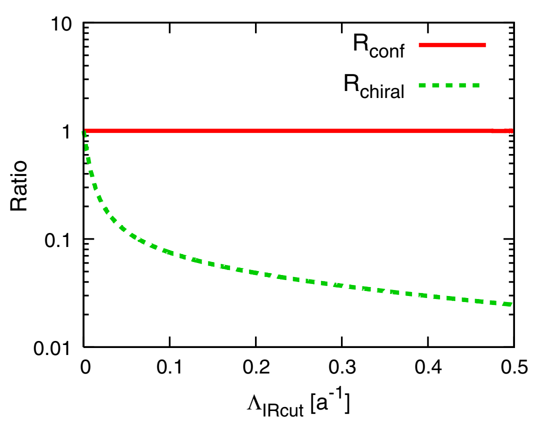

FIG. 5 (color online). The numerical results for the R_{chiral} and R_{conf} ratio from Eqs. (38) and (39), respectively, as a function of an infrared cutoff Λ introduced on Dirac eigenvalues, expressed in lattice units. The Monte Carlo calculations have been performed on the $10^3 \times 5$ lattice at $\beta = 5.6$ and for the quark mass of $m = 5$ MeV.

TABLE I. Numerical results for different Polyakov loop fluctuations (original) and those without the low-lying Dirac modes (IR removed) below the IR cutoff $\Lambda \simeq 0.4$ GeV. The results are obtained in quenched QCD on the $10^3 \times 5$ lattice at $\beta = 5.6$ (confined phase) and $\beta = 6.0$ (deconfined phase) with 20 gauge configurations.

β		Original	IR removed
$\beta = 5.6$	$T^3\chi_A$	3.475×10^{-4}	3.470×10^{-4}
	$T^3\chi_L$	5.307×10^{-4}	5.298×10^{-4}
	$T^3\chi_T$	6.005×10^{-4}	5.994×10^{-4}
	R_A	0.6548	0.6549
	R_T	1.131	1.131
$\beta = 6.0$	$T^3\chi_A$	2.965×10^{-3}	2.965×10^{-3}
	$T^3\chi_L$	3.015×10^{-3}	3.015×10^{-3}
	$T^3\chi_T$	7.848×10^{-4}	7.848×10^{-4}
	R_A	0.9834	0.9834
	R_T	0.2603	0.2603

cutoff Λ. For the sake of comparison, we also show in Fig. 5 the R_{chiral} ratio, calculated at the same temperature and with the light quark mass, $m = 5$ MeV. The ratios, R_{conf} and R_{chiral}, indicate the influence of removing the low-lying Dirac modes with the infrared cutoff Λ on confinement and chiral symmetry breaking, respectively.

From Fig. 5, it is clear that the R_{chiral} ratio is strongly reduced by removing the low-lying Dirac modes. Thus, the low-lying Dirac modes, which are important modes for chiral symmetry breaking, are also dominant to quantify the chiral condensate. In contrast to R_{chiral}, the R_{conf} ratio is almost unchanged when removing the low-lying Dirac modes even with relatively large cutoff $\Lambda \simeq 0.5$ GeV.

Thus, the essential modes for chiral symmetry breaking in QCD are not important to quantify the Polyakov loop fluctuation ratios, which are sensitive observables to confinement properties in QCD. The same result is also found in the deconfined phase, as seen in Table I, which summarizes our numerical results on different fluctuations of the Polyakov loop and their ratios, obtained on the lattice at $\beta = 5.6$ and $\beta = 6.0$, with 20 gauge configurations. Note here that the analytical relation (20) and the subsequent formulas of Eqs. (27)–(29) hold for each gauge configuration, and the contribution from the low-lying Dirac modes to the Polyakov loop L is found to be negligible [26]. This fact inevitably leads to almost equivalence between the Polyakov loop fluctuations and those without the low-lying Dirac modes, although the statistical error is significant because of the small statistics.

The differences in the influence of the low-lying Dirac modes on the chiral condensate and the Polyakov loop fluctuations can be understood semianalytically. From Eqs. (27)–(29), it is clear, that the contribution of the low-lying Dirac-modes with $|\lambda_n| \simeq 0$ is suppressed, relative to the higher-lying Dirac modes, due to the damping factor $\lambda_n^{N_\tau - 1}$. In fact, a Dirac matrix element $\langle n|\hat{U}_4|n\rangle$ does not yield a stronger singularity than $1/\lambda_n^{N_\tau - 1}$; therefore, the contribution from the low-lying Dirac modes to the Polyakov loop [26], as well as to its fluctuations, is negligible. Hence, the essential modes for chiral symmetry breaking do not contribute to a sensitive probe for deconfinement in QCD. Thus, this finding suggests no direct one-to-one correspondence between confinement and chiral symmetry breaking in QCD.

V. SUMMARY AND CONCLUSIONS

The main objective of these studies was to establish the relation between the Polyakov loop and its fluctuations with the eigenmodes of a Dirac operator. Based on the lattice QCD formalism, we have derived a Dirac spectral representation of the real and imaginary parts and modulus of the Polyakov loop and their fluctuations. Although the formulation was done on a temporally odd-number lattice, this choice of the parity for the lattice size does not alter the physics in the continuum limit with any large number of N_τ. The analytical decomposition of the Polyakov loop and its fluctuations is fully general. It is independent from the gauge group, the implementation of fermions on the lattice, and is also valid at a finite baryon density.

To quantify the influence of Dirac modes over the Polyakov loop fluctuations, we have performed Monte Carlo simulations in the SU(3) lattice QCD. Our calculations were carried out with the standard plaquette action at the quenched level on a $(10^3 \times 5)$-size lattice at two different temperatures, corresponding to the confined and deconfined phases.

We have shown that the low-lying Dirac modes have a negligible contribution to the Polyakov loop fluctuations. This result is intact both in the confined and deconfined phases. On the other hand, the low-lying Dirac modes are essential, in both phases, to quantify the chiral condensate.

These findings, both in analytical formulas and in numerical calculations, suggest no direct, one-to-one correspondence between confinement and chiral symmetry breaking in QCD. However, this does not exclude a coincidence of these two properties in QCD since the abrupt change of the ground state from the chiral broken phase to the restored phase may drive the onset of deconfinement.

The above conclusion is based on the numerical simulations on a rather small-size lattice, being far from a continuum limit. Thus, our result on the Polyakov loop fluctuations suffers from finite size effects. Such effects can certainly modify the values of fluctuations at a given temperature but will not change our conclusion on the influence of the low-lying Dirac modes on their properties. The low-lying Dirac modes have a negligible contribution to the Polyakov loop fluctuations because of the damping factor $\lambda_n^{N_\tau-1}$ which appears in Eq. (20). Although our numerical calculation was performed at the quenched level, the derived analytic formulas are fulfilled even in the presence of dynamical quarks. It is one of the future prospects to perform full-QCD simulations in the present formalism to further justify our conclusion.

In addition, the derived analytic relations connecting the Polyakov loop and Dirac modes are mathematically exact for arbitrary odd temporal size N_τ. Thus, we expect that our conclusion is rather robust in the continuum limit [25,26]. Moreover, the ambiguity of the multiplicative renormalization of the Polyakov loop has been avoided in the ratio of the Polyakov loop susceptibilities. Yet, it is left as an important but difficult task to extrapolate these analytic relations to the continuum.

In addition to the Polyakov loop fluctuations, there are further observables which are linked to deconfinement properties in QCD and show an abrupt, but smooth, change across the chiral crossover. One of such observables is the kurtosis of the net-quark number fluctuations [37–39]. Besides, the QCD monopole, in the maximally Abelian gauge, is a relevant degree of freedom in the low-energy QCD [20,21] and plays a fundamental role for nonperturbative phenomena such as confinement and chiral symmetry breaking. Thus, from the future perspectives, it would be of particular interest to investigate such quantities in terms of the Dirac-mode expansion and to explore the influence of the low-lying eigenmodes on their properties near the chiral crossover.

ACKNOWLEDGMENTS

K. R. acknowledges partial support of the U.S. Department of Energy under Grant No. DE-FG02-05ER41367, and fruitful discussions with Bengt Friman and Pok Man Lo. T. M. D. is supported by Grant-in-Aid for JSPS Fellows (Grant No. 15J02108), and H. S. is supported by the Grants-in-Aid for Scientific Research (Grant No. 15K05076) from Japan Society for the Promotion of Science. The work of K. R. and C. S. has been partly supported by the Polish Science Foundation (NCN) under Maestro Grant No. DEC-2013/10/A/ST2/00106 and by the Hessian LOEWE initiative through the Helmholtz International Center for FAIR. The lattice QCD calculations were performed on NEC-SX8R and NEC-SX9 at Osaka University.

[1] Y. Nambu and G. Jona-Lasinio, Phys. Rev. **122**, 345 (1961); **124**, 246 (1961).

[2] J. B. Kogut and L. Susskind, Phys. Rev. D **11**, 395 (1975).

[3] M. Creutz, *Quarks, Gluons and Lattices* (Cambridge University Press, Cambridge, England, 1985); H. J. Rothe, *Lattice Gauge Theories* (World Scientific, Singapore, 2012), and references therein.

[4] J. Greensite, *An Introduction to the Confinement Problem* (Springer, Berlin, 2011), and references therein.

[5] K. Fukushima and C. Sasaki, Prog. Part. Nucl. Phys. **72**, 99 (2013).

[6] Y. Nambu, Phys. Rev. D **10**, 4262 (1974); G. 't Hooft, *Proceedings of the International Conference on High Energy Physics, Palermo, Italy, 1975* (Editrice Compositori, Bologna, 1976); S. Mandelstam, Phys. Rep. **23**, 245 (1976).

[7] V. Gribov, Nucl. Phys. **B139**, 1 (1978); D. Zwanziger, *ibid.* **B323**, 513 (1989).

[8] T. Kugo and I. Ojima, Prog. Theor. Phys. Suppl. **66**, 1 (1979).

[9] G. Boyd, J. Engels, F. Karsch, E. Laermann, C. Legeland, M. Lutgemeier, and B. Petersson, Phys. Rev. Lett. **75**, 4169 (1995).

[10] G. Boyd, J. Engels, F. Karsch, E. Laermann, C. Legeland, M. Lutgemeier, and B. Petersson, Nucl. Phys. **B469**, 419 (1996).

[11] S. Borsanyi, G. Endrodi, Z. Fodor, S. D. Katz, and K. K. Szabo, J. High Energy Phys. 07 (2012) 056.

[12] P. M. Lo, B. Friman, O. Kaczmarek, K. Redlich, and C. Sasaki, Phys. Rev. D **88**, 014506 (2013).

[13] P. M. Lo, B. Friman, O. Kaczmarek, K. Redlich, and C. Sasaki, Phys. Rev. D **88**, 074502 (2013).

[14] F. R. Brown, F. P. Butler, H. Chen, N. H. Christ, Z. Dong, W. Schaffer, Leo I. Unger, and Alessandro Vaccarino, Phys. Rev. Lett. **65**, 2491 (1990).

[15] Y. Aoki, G. Endrodi, Z. Fodor, S. D. Katz, and K. K. Szabo, Nature (London) **443**, 675 (2006).

[16] A. Bazavov *et al.*, Phys. Rev. D **85**, 054503 (2012).

[17] T. Banks and A. Casher, Nucl. Phys. **B169**, 103 (1980).

[18] F. Karsch, Lect. Notes Phys. **583**, 209 (2002), and references therein.

[19] J. D. Stack, S. D. Neiman, and R. J. Wensley, Phys. Rev. D **50**, 3399 (1994).

[20] O. Miyamura, Phys. Lett. B **353**, 91 (1995).

[21] R. M. Woloshyn, Phys. Rev. D **51**, 6411 (1995).

[22] H. Suganuma, A. Tanaka, S. Sasaki, and O. Miyamura, Nucl. Phys. B, Proc. Suppl. **47**, 302 (1996).

[23] C. B. Lang and M. Schrock, Phys. Rev. D **84**, 087704 (2011); L. Ya. Glozman, C. B. Lang, and M. Schrock, Phys. Rev. D **86**, 014507 (2012).

[24] S. Gongyo, T. Iritani, and H. Suganuma, Phys. Rev. D **86**, 034510 (2012); T. Iritani and H. Suganuma, Prog. Theor. Exp. Phys. **2014**, 033B03 (2014).

[25] H. Suganuma, T. M. Doi, and T. Iritani, arXiv:1404.6494; *Proc. Sci.*, Lattice2013 (2013) 374; QCD-TNT-III2014 (2014) 042; Eur. Phys. J. Web Conf. **71**, 00129 (2014); *Proc. Sci.*, Hadron 2013 (2014) 121.

[26] T. M. Doi, H. Suganuma, and T. Iritani, Phys. Rev. D **90**, 094505 (2014); *Proc. Sci.*, Lattice 2013 (2013) 375; Hadron 2013 (2014) 122.

[27] C. Gattringer, Phys. Rev. Lett. **97**, 032003 (2006); F. Bruckmann, C. Gattringer, and C. Hagen, Phys. Lett. B **647**, 56 (2007).

[28] F. Synatschke, A. Wipf, and K. Langfeld, Phys. Rev. D **77**, 114018 (2008).

[29] E. Bilgici, F. Bruckmann, C. Gattringer, and C. Hagen, Phys. Rev. D **77**, 094007 (2008).

[30] Y. Aoki, Z. Fodor, S. D. Katz, and K. K. Szabo, Phys. Lett. B **643**, 46 (2006).

[31] A. Bazavov *et al.* (HotQCD Collaboration), Phys. Rev. D **90**, 094503 (2014).

[32] Y. Aoki, S. Borsanyi, S. Durr, Z. Fodor, S. D. Katz, S. Krieg, and K. K. Szabo, J. High Energy Phys. 06 (2009) 088.

[33] T. Bhattacharya *et al.* Phys. Rev. Lett. **113**, 082001 (2014).

[34] S. Elitzur, Phys. Rev. D **12**, 3978 (1975).

[35] E. Anderson *et al.*, *LAPACK Users' Guide*, 3rd ed. (Society for Industrial and Applied Mathematics, Philadelphia, 1999).

[36] M. Creutz and K. J. M. Moriarty, Phys. Rev. D **26**, 2166 (1982).

[37] S. Ejiri, F. Karsch, and K. Redlich, Phys. Lett. B **633**, 275 (2006).

[38] C. Schmidt (BNL-Bielefeld Collaboration), Nucl. Phys. **A904–A905**, 865c (2013).

[39] C. Sasaki, Nucl. Phys. **A931**, 238 (2014).